Investigation of the influence of capillary effect on operation of the loop heat pipe

DARIUSZ MIKIELEWICZ*
KRZYSZTOF BŁAUCIAK

Gdańsk University of Technology, Faculty of Mechanical Engineering,
Narutowicza 11/12, 80-233 Gdańsk, Poland

Abstract   In the paper presented are studies on the investigation of the capillary forces effect induced in the porous structure of a loop heat pipe using water and ethanol ad test fluids. The potential application of such effect is for example in the evaporator of the domestic micro-CHP unit, where the reduction of pumping power could be obtained. Preliminary analysis of the results indicates water as having the best potential for developing the capillary effect.

Keywords: Loop heat pipe; Capillary forces; Waste heat recovery

1   Introduction

Loop heat pipes (LHPs) have been extensively investigated for space applications towards the thermal control of satellites and components. As a reliable two-phase passive thermal control device, large amounts of heat can be managed with a good control of the heat source temperature. LHPs operate passively by means of capillary forces generated in the evaporator and its design needs special attention as it is coupled with the compensation chamber, which is responsible for establishing the loop's operation temperature and self-regulates the working fluid inventory during the LHP operation. Several applications of LHPs have already shown their thermal control capability in space environments, Launay [1].

---

*Corresponding Author. E-mail: Dariusz.Mikielewicz@pg.gda.pl

The new promising direction of application of the general idea of LHP is the modern dispersed energy sector development, and in particular applications utilizing cogeneration and recovery of waste heat. One of such examples that could in future supplement the centralized energy sector is the microheat and power unit (micro-CHP) operating according to the Clausius-Rankine cycle with organic fluid (ORC) [2,3]. In such system the heat produced by the boiler can be used for central heating and the utility hot water for domestic use, but as a byproduct electricity can also be generated, which can be used on site or sold to the grid. The source of heat for such micro-power plant, in relation to the local capabilities, can be the fossil fuel or renewable sources of energy. Such heat in the micro-power plants is better used than in professional power plants producing electricity only.

As the capillary evaporator and the compensation chamber form only one component in the LHP, their design must be carefully carried out to promote the desirable device operation. In the paper presented is the experimental facility designed for studies of the capillary effect in porous media for further implementation in LHPs together with the results of commissioning tests. Examined are two fluids, namely ethanol and water, at three different fillings and three different evaporator temperatures. The results in the form of pressure distribution with time have been presented.

2   Experimental facility

The most complicated parts of LHP are the evaporator and compensation chamber, which are most of the times configured to be present in one containment, as the compensation chamber usually is directly prior to the evaporator. The wick structure is responsible for the transport of working fluid in the loop. The wick is usually made of high quality sintered porous powders to induce the capillary pressure difference indispensable for self excited working fluid circulation in the loop. In our analysis we are going to consider the arrangement presented in Fig. 1. The principle of operation of the loop heat pipe is relatively simple. The heat is supplied to the preheater and the evaporator where the working is intended to reach saturation state (preheater) and subsequently evaporate (evaporator). The working fluid forms a meniscus at the contact surface between liquid and vapor in the wick structure. Arising capillary forces in the form of capillary pressure push out vapour in the direction of condenser rendering the fluid transport around the loop. It ought to be stressed that no circulation pump is needed
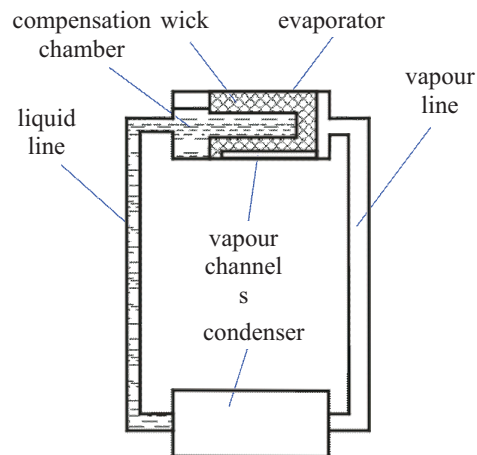
Figure 1: Principle of operation of the loop heat pipe.

in such arrangement. The compensation chamber serves for storing and sustaining of the surplus of working fluid and control of LHP operation. As can be noticed the only form of energy required to be supplied to the device is the thermal energy. As such the waste energy can be considered and that opens significant potential for other applications. The primary wick in the evaporator must produce the capillary pressure necessary to overcome the total pressure drop in the loop sustaining in such way the continuous operation of the LHP.

To take the advantage of capillary forces for aiding of the working fluid pumping in the foreseen domestic micro-CHP facility, it is assumed that in the perspective CHP arrangement evaporator will be a shell and tube recuperator, in which tubes will be made of sintered metal powder in the form of a porous tubular wick. Porous material will transport the working fluid from the inner to the outer surface of the wick, from where it will be evaporated and transported further to turbine. The presence of the wick will cause a reduction of pressure head demand for pumping of the working fluid. The evaporator collector that feeds the working fluid to evaporator tubes will additionally serve as a compensation chamber. The preheater present in Fig. 2 heats the working fluid up to saturation temperature. Structural scheme of this cycle is shown in Fig. 2 [4].

Due to the fact that the fundamental element as well as the topic of present investigations is the tube with porous filling referred to later as heat exchanger which utilizes capillary pressure difference arising in the porous
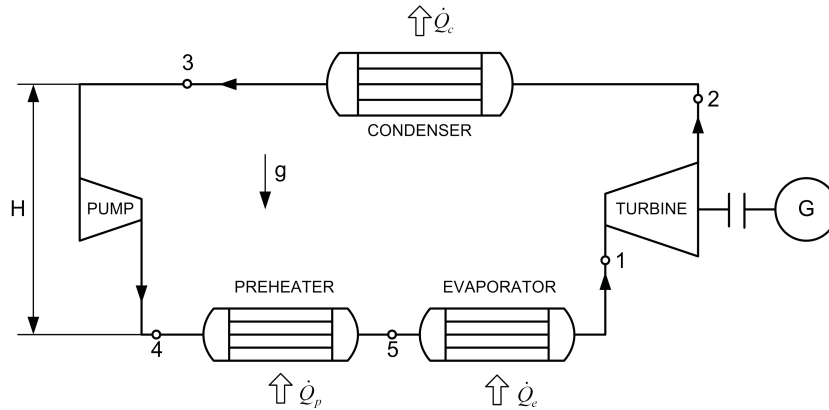
Figure 2: Structural scheme of the ORC cycle.

structure the activities started with selection of the appropriate structure of the tube with the porous filling. The required porous tube to be used in LHP evaporator is made of sintered stainless steel powder AISI 316L, which results in a fully permeable porous wick featuring the mean pore structure of 1, 3 and 7 μm, bearing the commercial name of Siperm (sintered permporous). The cross-section of the material sample made of stainless steel powder, characteristic for a very high adsorption coefficient due to irregular shape of powder grain is presented in Fig. 3. The implemented technology for obtaining such porous structure is named the technique of isostatic pressing. AISI 316L is a stainless steel with elevated corrosion resistance in aggressive environment. It enables operation in temperatures reaching 300/400 °C.

Figure 3: Sample of SIPERM R3 [5].

Selection of stainless steel as the material of the test section was dictated primarily by the two most important assumptions made for the study. The first objective of the study was to be able to carry out research with different working fluids such as water, ethanol, hydrofluorocarbons without the problems of material damage/corrosion. Actually stainless steel renders it possible to work with most of working fluids [6]. The second fundamental criterion was the possibility of mechanical and thermal processing of the wick structure. Bearing in mind these constraints the porous tube connected by welding with the stainless steel flange was developed, Fig. 4. The porous tube is closed on one end with the plate made of Siperm to separate the high and low pressure zones of the arrangement, whereas the other end was welded to the flange to be able to position the tube within the internally grooved tube, named evaporator.
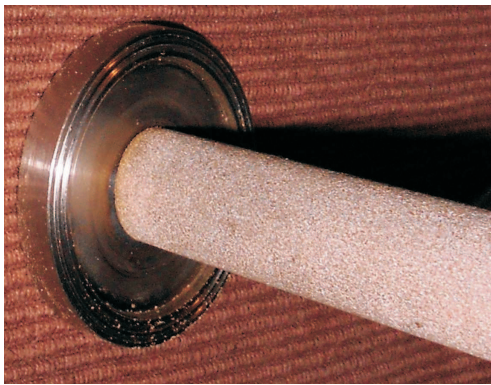

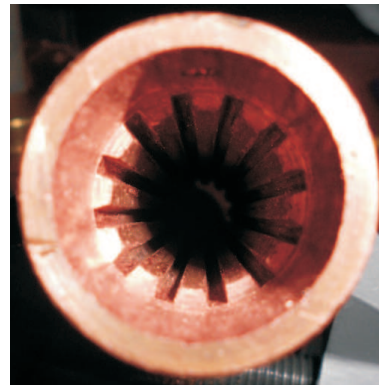Figure 4: Welded connection of the wick with the flange.

Figure 5: Grooves on internal side of the copper tube.

Another challenge in the development of the test section of the experimental facility, requiring implementation of advanced processing technique, was the body of the evaporator. The technology of production of the wick on the basis of permeable porous tube disabled cutting of the grooves on its external surface. These grooves are necessary to transport away the produced vapor. Such grooves cut in the porous material are characteristic to the studies by Chernysheva and Maydanik [7], Bai *et al.* [8] or Hartenstine *et al.* [9]. In order to alleviate that problem the groves were cut inside the tube serving as the casing for evaporator. The tube was made of copper M1E by means of the wire electro-erosion machine with the accuracy of 0.01 mm, Fig. 5.

The volume of the compensation chamber (CC) was experimentally adjusted. The CC was connected with the evaporator by means of special Teflon labyrinth sealings assuring the adequate tightness and possibility of nondamaging inspections of the inside chamber of the evaporator, wick and compensation chamber. The view of the connection between the compensation chamber and the evaporator is shown in Fig. 6.
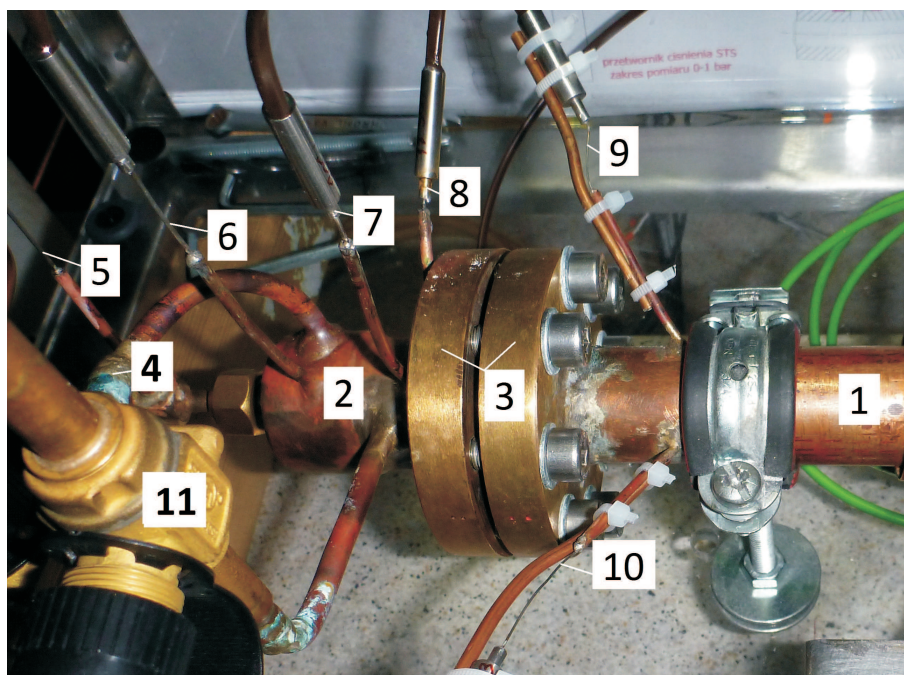

Figure 6: View of the connection between the compensation chamber and the evaporator; 1 – evaporator casing, 2 – compensation chamber, 3 – flange connection between cmpensation chamber and evaporator, 4 – filling/emptying socket, 5 – thermocouple T12, 6–10 – thermocouples T1–T5, 11 – cut-off valve for pressure transducer P1.

Transport lines connecting the evaporator to condenser were made of capillary tubes with internal diameters of 1.95 mm in case of the vapour line and 1.8 mm in case of the liquid line. Cooling of the condenser section was accomplished by means of water circulating in a closed loop by the circulation pump providing the flow rate up to about 0.175 dm^3/min. The test facility was also equipped with the visualisation section. To accomplish that applied were the two-way valves enabling to direct the flow of working fluid from the copper capillary tube to the transparent glass tube made of

borium-silicone glass. The source of heat necessary to induce the process of heat transport in the wick in the form of capillary pressure difference was obtained by application of a heating wire of 400 W duty allowance installed in the middle part of the evaporator casing. Uniform radial supply of heat to the wick was assumed. The supply of electric current was controlled by the proportional-integral-derivative (PID) controller in relation to the temperature on the contact surface between the heating element and the evaporator casing.

The measurement system of the facility consists of the following instrumentation:

- pressure; accomplished by the set of 4 pressure transducers with the measurement range 0–1 MPa of absolute pressure and measurement class of 0.1. The transducers are integrated to digital displays AR500. Exact locations of transducers enable pressure readings in the nodes provided by Tab. 1;

- temperature; set of 18 T-type thermocouples manufactured in the class 1 accuracy connected to temperature meters EMT200 with measurement error equal to $\pm(0.002x$ [T] $+ 0.3$ °C $+$ number) integrated with multiplexer PMP201. Locations of thermocouples are shown in Tab. 2;

- electric power; multimeter UT71E with measurement accuracy $\pm(2\%$ $+50)$ recording the electrical power demand through the resistance heated wire generating the rate of heat supplied to the evaporator section.

Table 1: Locations of pressure readings.

Symbol	Location of pressure measurement points pressure transducer type STS ATM.ECO (allowed temperature range -40–150 °C):
P1	compensation chamber
P2	vapour space beyond the wick
P3	transition of the vapour line into condenser section
P4	transition of condensation section into the liquid line

In order to reduce the heat dissipation from the test facility the heating section, buffer tank with tappings and thermocouples were insulated using

Table 2: Locations of temperature readings.

Symbol	Location of the temperature measurement points Thermocouples type T - 100% Cu (temperature range -100–400 °C):
T1	working fluid – compensation chamber
T2	working fluid – compensation chamber
T3	working fluid – inside wick
T4	working fluid – vapour groove
T5	working fluid – vapour groove
T6	working fluid – vapour groove
T7	working fluid – outlet from evaporator in vapour
T8	casing of evaporator/heater contact
T9	working fluid – inlet to vapour line
T10	working fluid – outlet from vapour line
T11	working fluid – inlet to liquid line
T12	working fluid – outlet from liquid line
T13	water supply to condensation section
T14	water return from condensation section
T15	water in the buffer tank
T16	inside the research rig
T17	surroundings
T18	contact between evaporation casing and heater – PID control

mineral wool with aluminium coating. The vapour line and liquid lines were insulated using the synthetic rubber of 13 mm thickness, Fig. 7. Technical parameters of the research facility for loop heat pipe investigations have been gathered in Tab. 3.

As it was mentioned earlier the objective of investigations was to determine the capabilities of the facility to transport heat and mass through implementation in the pumpless arrangement of the porous structure with known parameters. The testing procedure considered tests at three different levels of filling the installation with working fluid. In the light of the lack of necessary information about it the knowledge from refrigeration technology about the refrigeration installation filling was assumed. Another considered aspect of investigations which was attempted to be identified was the influence of the working fluid selection, installation filling and different levels of heat supply on the transport capabilities of the heat exchanger at the
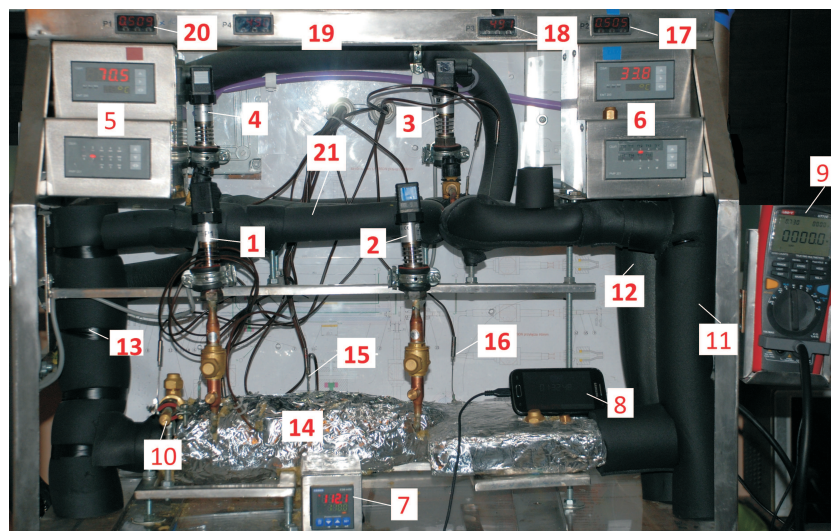
a)
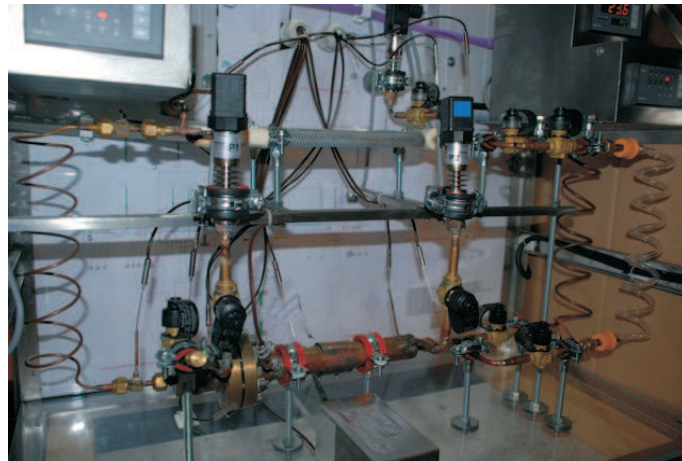
b)

Figure 7: View of the experimental facility: a) without necessary insulation of evaporator, vapour and liquid lines; b) with insulations: 1–4 – pressure transducers P1–P4, 5 – temperature reader for thermocouples T1–T9, 6 – temperature reader for thermocouples T10–T18, 7 – PID regulator – heater mains supply, 8 – time recorder, 9 – electric power recorder, 10 – filling/emptying socket, 11 – insulated vapour line made of borium-silicone glass, 12 – insulated vapour line made of copper, 13 – insulated liquid line made of copper, 14 – insulated evaporator and compensation chamber, 15 – resistance heater, 16 – thermocouple T9, 17–20 –display from pressure transducers P2, P3, P4 and P1 respectively, 21 – insulated condenser section.

Table 3: Technical parameters of the facility for LHP.

No.	Name of measurement with description	Unit	Value of parameter
1.0	Working fluid – type	name	water, ethanol
1.1	Filling	g	60, 65, 70
1.2	Total volume of the facility	ml	100
2.0	Wick – type		sintered material/cylinder
2.1	Material		AISI 316L
2.2	Number of wick layers		one layer
2.3	Application of bayonet		yes
2.4	Angle of capillaries	μm	2.8
2.5	Max angle of capillaries	μm	3.0
2.6	Porosity	%	33.0
2.7	Coefficient of laminar flow	m^2	1*10<-12
2.8	Coefficient of turbulent flow	m^2	1*10<-7
2.8	Max thermal conductivity of the wick material	W/mK	10.2 at 20 °C
2.9	Outer wick diameter OD	mm	18.0
2.10	Inner wick diameter ID	mm	8.0
2.11	Wick wall thickness	mm	5.0
2.12	Wick length	mm	200.0
2.13	Volume of wick inside space	ml	49.62
2.14	Crossection of vapour grooves	mm	2x2 inside tube
2.15	Number of vapour grooves	–	12
2.16	Length of vapour grooves	mm	198.0
2.17	Radial permeability in saturation	W/K	9.6 – 10.2
3.0	Compensation chamber – type		cylinder
3.1	Material		Cu M1E
3.2	Chamber volume	ml	43.28
3.3	Chamber outer diameter OD	mm	35.0
3.4	Chamber inner diameter ID	mm	32.0
3.5	Inside length of the chamber	mm	49.5
4.0	Evaporator - type		cylinder
4.1	Material		Cu M1E
4.2	Outer diameter of evaporator casing OD	mm	31.0
4.3	Inner diameter of evaporator casing ID	mm	18.0
4.4	Thickness of evaporator wall	mm	6.5
4.5	Evaporator length	mm	216.5
4.6	Space at vapour outlet from evaporator	mm	20.0
4.7	Supply of heat to evaporator		electric resistance wire
4.8	Power of heat source	W	400 W, 230 V
5.0	Condenser – type		coil
5.1	Material		Cu
5.2	Outer diameter of condenser OD	mm	4.75
5.3	Inner diameter of condenser ID	mm	2.95
5.4	Thickness of condenser wall	mm	0.9
5.5	Length of condenser	mm	1430.0
5.6	Inner volume of condenser	ml	9.77
5.7	Condenser cooling		water jacket

6.0	Liquid line		capillary tubes
6.1	Material		Cu
6.2	Outer diameter of tubes OD	mm	3.2
6.3	Inner diameter of tubes ID	mm	2.0
6.4	Thickness of tube walls	mm	0.6
6.5	Length of line	mm	1152.4
6.6	Inner volume	ml	3.62
7.0	Vapour line		capillary tubes
7.1	Material		Cu
7.2	Outer diameter of tubes OD	mm	4.75
7.3	Inner diameter of tubes ID	mm	2.95
7.4	Thickness of tube walls	mm	0.9
7.5	Length of line	mm	880.0
7.6	Inner volume	ml	6.02

assumption that the liquid and vapour lines were of the same length and the distance between the condenser and evaporator was also the same. The latter assumption leads to the same level of hydrostatic pressure in the installation. Due to the above restrictions the following range of experimental tests was set for scrutiny:

- 2 different working fluids, namely water and ethanol,

- 3 different porous structures with the pores size of 1, 3, and 7 μm,

- 3 different fillings of the installation, namely 60, 65, and 70 ml,

- 3 different values of evaporator casing temperature settings, namely $T_w = 90$, 100, and 110 °C.

Table 4 presents the whole range of investigated parameters together with attainable pressure differences. Accomplished experiments indicate the crucial issue of the adequate filling with the working fluid. For both fluids considered it was found that the pressure difference can reach up to 22 hPa for water as working fluid and the pore size of 1 μm at the installation filling of 65 ml. For other values of fillings significantly lower values of pressure difference have been obtained.

3   Results of experiments with one evaporator

During experiments four pressure readings were recorded, namely the ones in the compensation chamber, P1, vapour space beyond the wick, P2, before the condenser, P3, and after the condenser, P4. Recorded also were 18

Table 4: Range of investigated parameters.

No.	Filling volume, ml	Heater setting, °C	Working fluid	Pore size, μm	P_2–P_1, hPa
1	60	90, 100, 110	Water	R1	5
		90, 100, 110	Ethanol	R1	13
2	65	90, 100, 110	Water	R1	21
		90, 100, 110	Ethanol	R1	15
3	70	90, 100, 110	Water	R1	13
		90, 100, 110	Ethanol	R1	12
4	60	90, 100, 110	H_2O	R3	14
		90, 100, 110	Ethanol	R3	16
5	65	90, 100, 110	Water	R3	10
		90, 100, 110	Ethanol	R3	22
6	70	90, 100, 110	Water	R3	6
		90, 100, 110	Ethanol	R3	14
7	60	90, 100, 110	Ethanol	R7	5
8	65	90, 100, 110	Ethanol	R7	10
9	70	90, 100, 110	Ethanol	R7	8

temperature readings denoted in line with the Tab. 2. Here the discussion of the results will be done on the basis of the influence of different pore size and evaporator casing temperature on the attainable pressure difference. Presented will be the results for one value of the installation filling, namely 65 ml. For the case of water as working fluid the results are presented in Figs. 8 to 10, whereas in the case of ethanol in Figs. 11 to 13.

3.1   Water as working fluid

Analysis of pressure distributions for particular measurements in case of water as working fluid indicates that the pressure drops in the liquid and vapour lines are small in comparison to the pressure difference before and after the evaporator P2 (pressure after the evaporator and compensation chamber) is the highest pressure in installation and P1 (pressure before compensation chamber) is the lowest pressure in installation). In all distributions of pressure significant pressure fluctuations are observed. During investigations, in which the measurement series lasted for about 2.5 h we can observe that the first half an hour is the time of reaching the steady state conditions. In case of experimental run presented in Fig. 8a that means that the rate of pressure increase is about 445 Pa/s. In authors opinion the subsequent pressure fluctuations can be explained by the fact that pro-
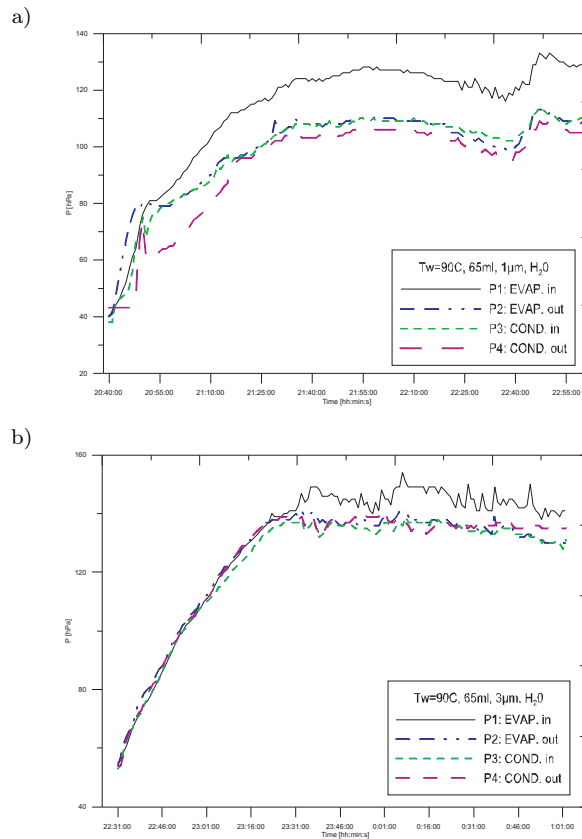
a)

b)

Figure 8: Pressure distribution in function of time in four specific nodes of installation. Working fluid – water, $T_w = 90\,^{\circ}$C, filling volume 65 ml, pore size: a) $d_p = 1\,\mu$m, b) $d_p = 3\,\mu$m.

duction of vapour in the grooves can contribute to choking of the porous structure. It ought to be stressed that in all runs the steady state conditions are reached after about 30 min of the experiment duration. In the case of research with water as working fluid the initial installation pressure was at the level of 40 hPa. The supply of heat rendered the pressure increase. In case of the parameters corresponding to the run presented in Fig. 8a the pressure in the compensation chamber P1 stabilised at the level of 130 hPa, whereas the pressure in the vapour line at 105 hPa. From that pressure difference results the characteristics of the evaporator wick. In the case of the considered experiment that is equal to 25 hPa for the temperature of evaporator casing of 90 $^{\circ}$C and the pore size of 1 μm. In the case of the

experiment presented in Fig. 8b where in relation to the data presented in Fig. 8a the size of the pore is increased from 1 to 3 μm the pressure P1 stabilises at the level of 140 hPa, whereas the pressure in the vapour channel is 130 hPa. That confirms the fact that the reduction of the pore size leads to the increase of produced pressure. In case of the evaporator casing temperature of 90 °C that is 5 hPa.
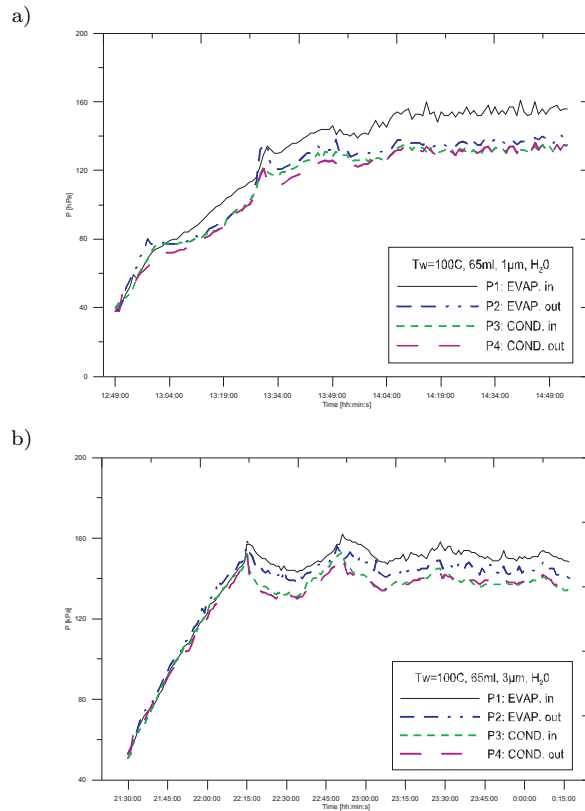

Figure 9: Pressure distribution in function of time in four specific nodes of installation. Working fluid-water, $T_w = 100$ °C, filling volume 65 ml, pore size a) $d_p = 1\,\mu$m, b) $d_p = 3\,\mu$m.

In Fig. 9 the similar situation to that presented in Fig. 8 holds, however the evaporator casing temperature now is equal to 100 °C. At the filling volume of 65 ml the data for the pore size of 1 μm and 3 μm is presented. As can be seen from Fig. 9a the pressure in the compensation chamber is 157 hPa, whereas the pressure in the vapour line settles at 135 hPa. The

start-up time was 30 min. The pressure difference in the installation is hence 22 hPa. In case of the experiment with the pore size of 3 μm and the same evaporator casing temperature, Fig. 9b, the start-up time was 30 min and the pressure in the compensation chamber settled at the level of 150 hPa and 136 hPa in the vapour line. We can therefore see that the pressure difference in the installation is 14 hPa. It is significantly lower in relation the pressure difference from Fig. 9a, which again confirms the fact that with the increase of the pore size the potential to induce the capillary pressure difference decreases. There also should be noticed the fact that with the increase of evaporator casing temperature from 90 to 100 °C the potential to produce the capillary pressure difference decreases. Such conclusion can be drawn comparing the pressure distributions from Figs. 8a and 9a, where the difference between the cases is only in the setting of the evaporator casing temperature. In that case we have the pressure difference change of 3 hPa, which is the result of the change of the latter parameter. A similar situation holds in relation to the results presented in Figs. 8b and 9b. In case of data presented in Fig. 8b the pressure difference is 10 hPa, whereas in case of the data from Fig. 9b that is 14 hPa. In presentation of the data from Fig. 10 the temperature of the evaporator casing is set to 110 °C. In case of the data in Fig. 10a the pore size was equal to 1 μm, whereas in case of the data in Fig. 10b the pore size was equal to 3 μm. Also in these cases we can observe the start-up time equal to about 30 minutes prior to attaining the steady-state conditions. In case of data presented in Fig. 10a the time of experiment duration was not as long as before and that explains the qualitative difference in the results. In case of the data from Fig. 10b the pressure in the compensation chamber is 159 hPa and the pressure in the vapour line was 142 hPa, which renders the pressure difference in the installation equal to 17 hPa. In relation to the data from Fig. 8b and 9b that is the case of the largest pressure difference. The conclusion resulting from that is that at the constant size of the pore the increase of evaporator casing temperature renders the increase of the maximal pressure difference.

3.2 Ethanol as working fluid

The second analysed fluid was chemically pure ethanol. That is one of the fluids which can be considered in the perspective installation of the domestic micro-CHP, Mikielewicz and Mikielewicz (2010).

The analysis of pressure distributions for particular experimental runs is presented in Figs. 11–13. The general observation again is that the pressure
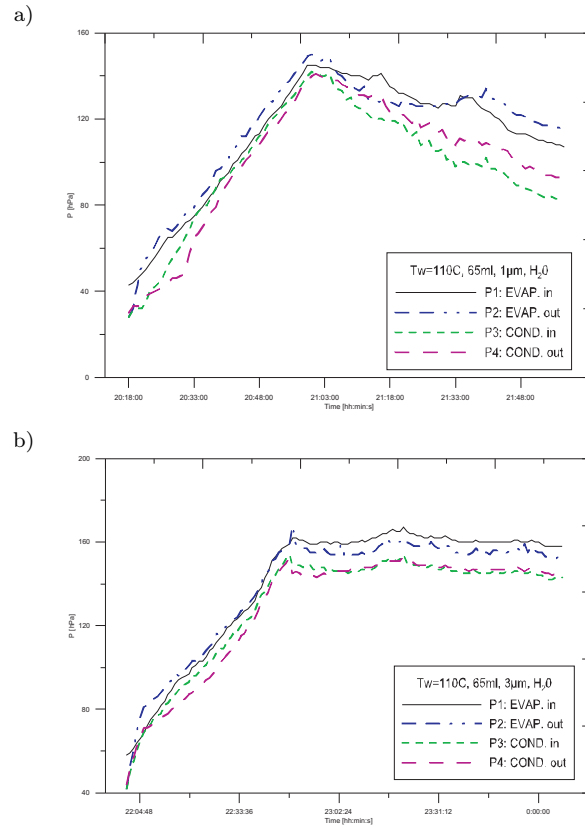
a)

b)

Figure 10: Pressure distribution in function of time in four specific nodes of installation. Working fluid-water, $T_w = 110\,^\circ$C, filling volume 65 ml, pore size a) $d_p = 1\,\mu$m, b) $d_p = 3\,\mu$m.

drops in the liquid and vapour lines are small in comparison to the pressure difference between the points before and after the evaporator. Another important observation is that the pressure fluctuations are generally smaller than in case of water as working fluid despite the fact that the operational pressure of the loop is much higher than in case of water. The experimental run lasted also for about 2.5 h and the first half an hour was related to the start-up, similarly as in the case of water as working fluid. The initial pressure in the installation is significantly different from the one present for the case of water. In case of filling of the installation with the volume of 65 ml of ethanol the initial pressure stabilized at the level of about 135 hPa, and due to the supply of heat the maximum pressure reached 302 hPa, for
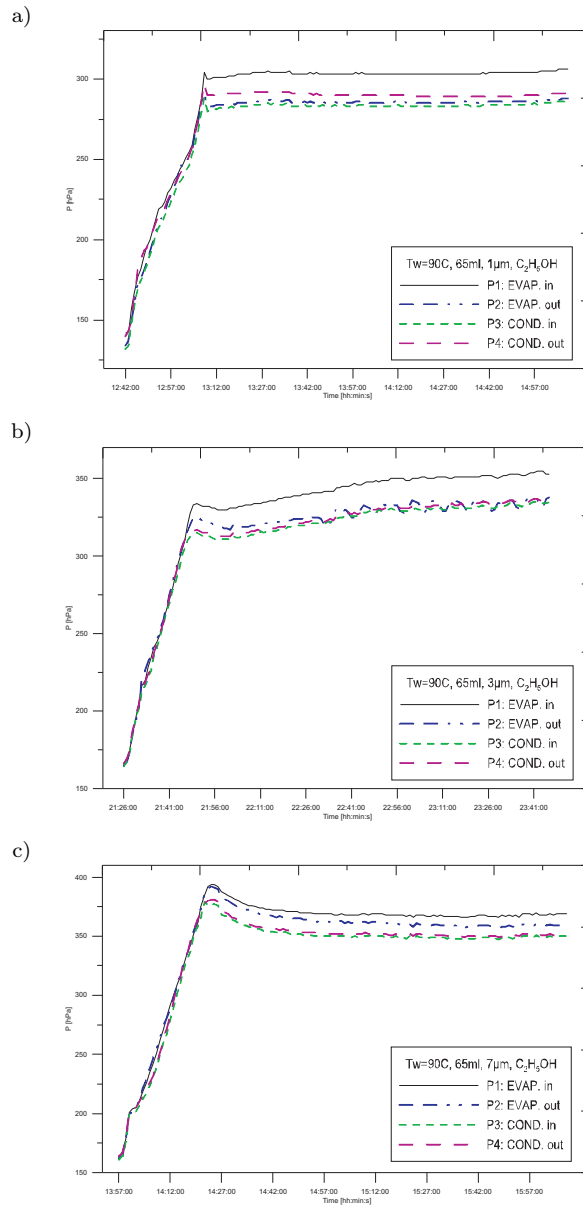
a)

b)

c)

Figure 11: Pressure distribution in function of time in four specific nodes of installation. Working fluid-ethanol, $T_w = 90$ °C, filling volume 65 ml, pore size a) $d_p = 1\,\mu$m, b) $d_p = 3\,\mu$m, c) $d_p = 7\,\mu$m.

the case of data from Fig. 11a. That corresponds to the rate of pressure change in the system equal to about 93 Pa/s. In case of other pore sizes as well as other evaporator casing temperatures the pressure reached values of 400 hPa. In case of the parameters corresponding to the Fig. 11a the pressure P1, pressure in the compensation chamber, settled at the level of 302 hPa, whereas the pressure in the vapour line at the level of 290 hPa. Therefore the wick produces the pressure increase of the order of 12 hPa for the temperature of evaporator casing equal 90 °C and the pore size of 1 μm. In the second case where the only difference to the setting from Fig. 11b is the pore size equal to 3 μm the pressure settled at the pressure of 351 hPa, whereas the pressure in the vapour channel at the level of 339 hPa, respectively. That conforms the fact that the reduction of the pore diameter leads to the increase of pressure. In the case of the evaporator casing temperature of 90 °C that is 12 hPa. In Fig. 11c presented have been the results for the case when the pore size is 7 μm. In that case the pressure in the facility stabilized at the level of 351 hPa, whereas the pressure in the vapour channel at the level of 336 hPa. We can see now that the size of pores has practically no influence on the attained capillary pressure difference. In Fig. 12 presented are the experimental results, where similarly to the case from Fig. 11 same pore sizes are compared but the temperature of evaporator casing is increased to 100 °C at the filling volume of 65 ml. As results from Fig. 12a the pressure in the compensation chamber is 320 hPa and the pressure in the vapour line is 299 hPa. The pressure difference is hence 21 hPa. In the case of the pore size equal to 3 μm, Fig. 12b, the start-up time was 30 minutes and the pressure in the compensation chamber settled at the level of 350 hPa, and in the vapour line at the level of 330 hPa, leading to the difference of pressure in the installation of 20 hPa. That pressure difference is smaller than in case of the pressure difference from Fig. 12a, which confirms the fact that with increase of the pore size the potential to produce capillary pressure difference decreases. In the case of pore size equal to 7 μm, Fig. 12c, the start-up time was 30 min and the pressure in the compensation chamber stabilized at the value of 370 hPa, and in the vapour line at the level of 350 hPa. In Fig. 13 presented are the results of investigations at the setting of evaporator casing temperature of 110 °C for three different pore sizes of 1 μm, 3 μm, and 7μm, respectively. A similar character of changes as in the case of evaporator temperature setting of 90 °C and 100 °C is present. It stems from the comparison of the three values of heater setting that with the increase of evaporator casing
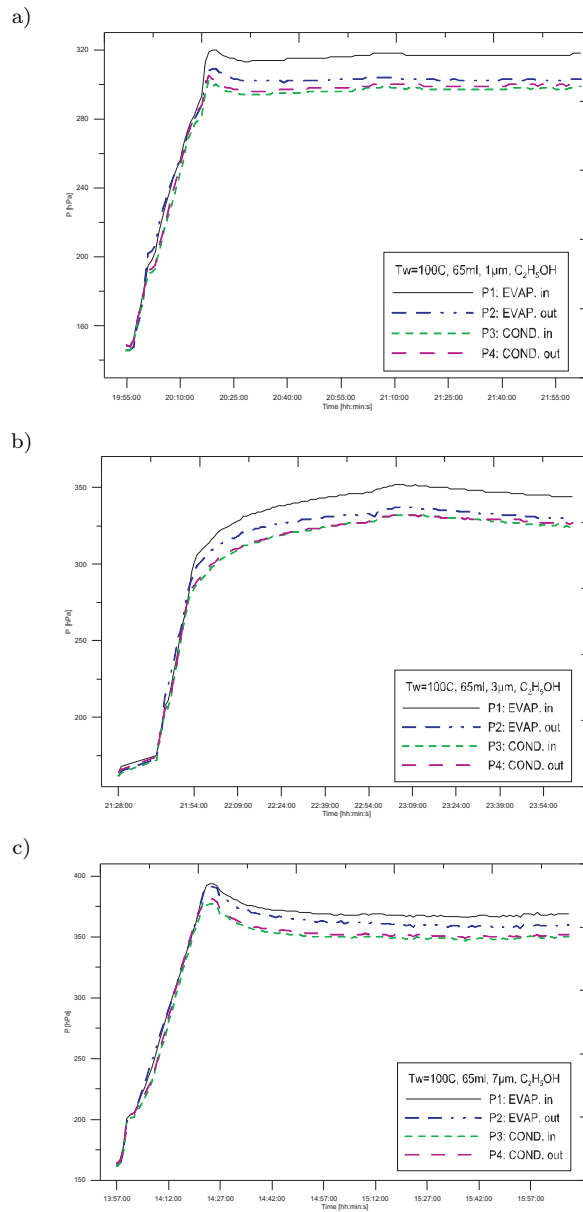
Figure 12: Pressure distribution in function of time in four specific nodes of installation. Working fluid-ethanol, $T_w = 100$ °C, filling volume 65 ml, pore size a) $d_p = 1\,\mu$m, b) $d_p = 3\,\mu$m, c) $d_p = 7\,\mu$m.

temperature, at the same value of the pore size, the potential to produce the capillary temperature difference decreases. Such conclusion can be drawn by comparing the Figs. 11a, 12a and 13a, where the pore size is 1 μm and the difference between these cases is only in the evaporator temperature setting Other comparisons at the same value of the pore size are in Figs. 11b, 12b, and 13b for the pore size of 3 μm respectively, and Figs. 11c, 12c, and 13c for the pore size of 7 μm. Due to the change of the setting of wall temperature the resulting pressure difference is 3 hPa.

4   Conclusions

The new facility for studies of capillary effect in the porous tube has been presented, namely the loop heat pipe rig. The facility has been developed to study the possibility of designing a innovative evaporator capable of reducing the pumping power requirement in the ORC installation. The net effect obtained in the facility was approximately 22 hPa in pressure difference has been obtained for studied porous material, namely the sintered tube from stainless steel powder with the average pore-size of 3 micrometers. That pressure difference can drive the fluid in the perspective heat exchanger. The topic will be further scrutinised with the view of testing other fillings of the tube, different other fluids, other pore sizes in the same material and finally by varying the vertical distance between the evaporator and condenser.

a)

b)

c)
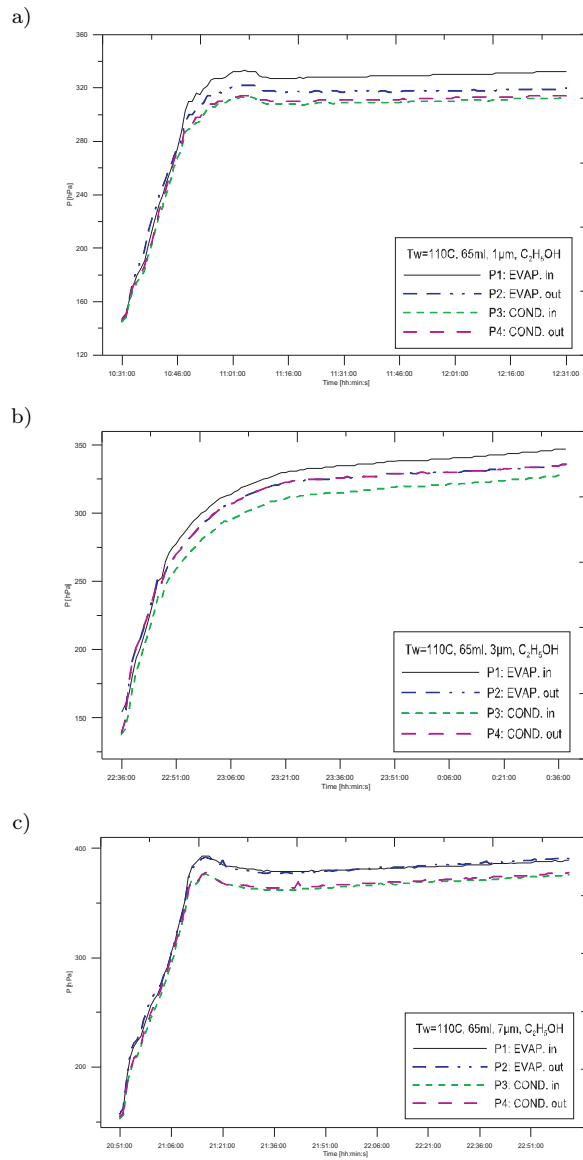

Figure 13: Pressure distribution in function of time in four specific nodes of installation. Working fluid-ethanol, $T_w = 110$ °C, filling volume 65 ml, pore size a) $d_p = 1\,\mu$m, b) $d_p = 3\,\mu$m, c) $d_p = 7\,\mu$m.

References

[1] LAUNAY S., VALLÉE M.: *State-of-the-art experimental studies on loop heat pipes.* Frontiers in Heat Pipes (FHP), 2, 013003 (2011), DOI: 10.5098/fhp.v2.1.3003.

[2] MIKIELEWICZ D., MIKIELEWICZ J.: *Cogenerative micro power plants – a new direction for development of power engineering?* Arch. Thermodyn. **29**(2008), 4, 109–132.

[3] MIKIELEWICZ D., MIKIELEWICZ J.: *The concept of capillary forces supported evaporator for application to domestic ORC unit.* Heat Transfer and Renewable Sources of Energy 2012, Międzyzdroje 2012.

[4] MIKIELEWICZ D., BŁAUCIAK K.: *Preliminary experimental results of the operation of the loop heat pipe facility.* XXI Int. Symp., Research-Education-Technology, Gdansk, 23-24 May, 2013.

[5] Promotion materials by Tridelta Spirem GmbH, Dortmund.

[6] FAGHRI A.: *Heat Pipe Science and Technology* Taylor & Francis Inc. 1995.

[7] CHERNYSHEVA M.A., MAYDANIK Y.F.: *Heat and mass transfer in evaporator of loop heat pipe.* J. Thermophys. Heat Transfer, **23**(2009), 4.

[8] BAI L., LIN G., ZHANG H., WEN D.: *Mathematical modeling of steady-state operation of a lop heat pipe.* Appl. Therm. Eng. **29**(2009), 2643–2654.

[9] HARTENSTINE J.R., ANDERSON W.G., BONNER R.: *Titanium Loop Heat Pipes for Space Nuclear Power System.* Space Technology and Applications International Forum-STAIF 2008.